Continuous single pass diafiltration with alternating permeate flow direction for high efficiency buffer exchange

Ruijie Tan, Fabian Hezel, Matthias Franzreb [*]

Institute of Functional Interfaces (IFG), Karlsruhe Institute of Technology (KIT), Eggenstein-Leopoldshafen, Karlsruhe, 76344, Germany

ABSTRACT

Looking at current trends within downstream processing (DSP) of high value bioproducts, it shows that there are ongoing efforts in replacing batch processes by continuous variants. However, a unit procedure which still lacks a simple and compact continuous variant is diafiltration. Here, we present such a single piece of diafiltration equipment achieving continuous buffer exchange of up to 99.90%. The device is composed of a 3D-printed single pass diafiltration (SPDF) module containing two commercial ultrafiltration membranes. While the retentate is flowing through a narrow channel between the two membranes, the channels above and below can supply diafiltration buffer or remove permeate solution. The obtained results illustrate systematically the vulnerability of the device to the effect of concentration polarization at the membrane surface, and that this problem can be strongly reduced using an alternating direction of diafiltration buffer perfusion through the membranes as process inherent backflush. By this, a quasi-stationary operation could be obtained during continuous diafiltration, making the device an interesting option for in-process buffer exchange.

1. Introduction

The production of high-quality biological products is widely becoming a key demand in the biomanufacturing industry. Batch processes, as the popular choice of the current commercial-scale production of biological products, are increasingly challenged by new, continuous process variants [1–3]. Several continuous process technologies, including perfusion bioreactors with continuous in- and outflow of materials, single pass tangential flow (SPTFF) units, continuous chromatography and continuous crystallization have been reported for multi-product clarification, purification and formulation [4–8].

There exist also recent developments exploring systems for continuous ultrafiltration (UF) and diafiltration (DF) [9–13]. Compared to conventional tangential flow filtration (TFF) in which the retentate is pumped in a loop and passes the membrane module several times, single pass tangential flow filtration (SPTFF) is more suitable for integration into continuous manufacturing schemes. As early as 2002, Lipnizki [14] and co-workers conducted a theoretical study of batch and continuous diafiltration of a protein solution using between two and ten plate-and-frame membrane modules. They compared three operation modes: (i) batch diafiltration with retentate recycling and all modules operation in parallel, (ii) continuous diafiltration with the retentate passing the modules sequentially and the admixture of diafiltration buffer between the stages, and (iii) continuous counter-current diafiltration injecting fresh diafiltration buffer only once in the final stage and always using the permeate as diafiltration solution of the proceeding stage. It showed that all three operation modes could reach the objective of 98% diafiltration efficiency, with the counter-current diafiltration requiring on the one hand more membrane area, but on the other hand, substantially less diafiltration buffer than the other operation modes. These results are in agreement with later findings reported in the literature [15] demonstrating that continuous counter-current multistage membrane processes result in better purification performances and reduced buffer requirements. However, the achieved purification factors and degrees of buffer exchange were relatively low, compared to the 99.9% diafiltration efficiency often required in biopharmaceutical processes. A first study approaching this limit was conducted by Rucker-Pezzini et al [6] showing the feasibility to obtain a buffer exchange greater than 99.75% using a three-stage single pass diafiltration (SPDF) process, with several repetitive steps of concentrating and diluting. In the same year also Nambiar and Zydney [16] demonstrated an around 350-fold impurity removal (corresponding to approximate 99.7% buffer exchange) applying a flow ratio of 19 between the diafiltration buffer and the feed (19 diavolumes) in a counter-current

two-stage single pass diafiltration system. The latest work reported by the same group exemplified a counter-current three-stage DF system by reconstructing the aforementioned two-stage DF system [17], which allowed to reduce the buffer consumption and accomplished up to 99.9% impurity removal. A different approach is the use of hollow fiber membrane systems originally designed for blood dialysis for counter-current diafiltration of protein solutions. Yehl et al. [18,19] applied a hollow fiber dialyzer for continuously removing the model impurity vitamin B_{12} from concentrated IgG solutions. They achieved around 1000-fold impurity removal at a very small buffer consumption between 2.25 - 4.5 diavolumes. However, to obtain these results the hollow fiber module had to operate at an unusually low specific feed rate of 0.16 L per m^2 of membrane area and hour. Nevertheless, to the knowledge of the authors, the approach of Yehl and Zydney is the first system achieving continuous, highly efficient diafiltration in a single device, which can be also realized as disposable.

In this work, we present an alternative design of a single pass membrane module, which can achieve comparable diafiltration efficiencies in a single device, however using common membrane sheets and specific feed rates, which are at least an order of magnitude higher than the ones in the mentioned hollow fiber modules. Different continuous DF modes, such as single-direction, alternating co-current and alternating counter-current, have been implemented in two 3D printed prototypes. In addition, the susceptibility to concentration polarization of the model protein at the membrane surface could be reduced to an acceptable level by implementing an alternating direction of the permeate flow through the membranes.

2. Material and methods

2.1. Feed solution and applied membrane

Bovine serum albumin (BSA) from PanReac AppliChem (Darmstadt, Germany) was used as the model protein in all experiments. BSA powder (1 g/L) was dissolved in 100 mM sodium chloride and 30 mM monosodium phosphate buffer at pH 7.10 (Merck KGaA, Darmstadt, Germany). The used ultrapure water was produced by a Sartorius arium® pro system (Sartorius, Gottingen, Germany). For buffer exchange, either ultrapure water or a diafiltration buffer containing 30 mM monosodium phosphate and 5 mM sodium chloride were used. The OMEGA ultrafiltration polyethersulfone (PES) membrane (30 kDa MWCO, OT030SHEET, Lot. #H3186I) purchased from Pall Life Sciences (Hauppauge, USA) was applied in the 3D-printed membrane modules as described in the next section.

2.2. Prototype and scaled-up 3D-printed UF/DF module

The continuous SPTFF experiments were carried out using two versions of a self-designed diafiltration module shown in Fig. 1. Both

modules were 3D printed using a PolyJet system EDEN 260 (Stratasys, Eden Prairie, USA.) using the material VeroWhite [20]. Each module was composed of two lateral parts and one middle part, all of them housing a narrow hollow-carved structure of 2 mm height allowing a tangential flow along the membranes placed between the parts. The grid-like design of the hollow-carved structure served at the same time as mechanical support for the two membranes. Bounded by these membranes, the middle part forms a channel in which the feed is transferred into the retentate during a single pass. During this passage diafiltration buffer can perfuse into the middle channel via one membrane while simultaneously permeate perfuses through the opposite membrane. Except for the flow path length, the structure of the three parts described was the same in the first prototype module (Fig. 1A) and the scaled-up module (Fig. 1B).

Table 1 below illustrates the main dimensions of the modules. Subtracting the area covered by the grid, the effective membrane area of the scaled-up module was 5.2-fold larger than the one of the prototype module. A longer flow path length was built in the scaled-up module in order to prolong the residence time of the retentate in the middle section, offering a practical way to improve the buffer exchange. Additionally, for the purpose of improving the leak tightness of the assembled module, narrow slots for rubber sealings were added on the inner side of the lateral parts in the scaled-up module.

2.3. Experimental set-up

Fig. 2 shows the developed experimental set-up for the continuous diafiltration process. The set-up combined the developed SPTFF module with two commercial systems: a FPLC system (AKTA purifier UPC 10, GE Healthcare, Uppsala, Sweden) including an additional sample pump and a membrane filtration system Sartorius (SARTOFLOW® Smart, Sartorius, Gottingen, Germany). This combination allowed a detailed and precise control of the operation conditions as well as an online monitoring of the main process parameters. The three high-pressure piston pumps of the FPLC system guaranteed a pressure independent control of the feed, diafiltration buffer, and retentate flows. The multiport valves of the FPLC system allowed an automated switching of the in- and outlet positions of the diafiltration and permeate flows. In addition, the system monitored the UV/Vis and conductivity signals in the retentate.

For the control of feed and retentate flows the feature of the Akta

Table 1
Dimensions of the two versions of the 3D-printed SPTFF module.

	A. Prototype module	B. Scaled-up module
$V_{lateral\ part}$ (ml)	1.25	6.46
$V_{middle\ part}$ (ml)	1.18	6.08
$L_{flow\ path}$ (cm)	4.70	24.5
$A_{effective,\ membrane}$ (mm^2)	532	2972
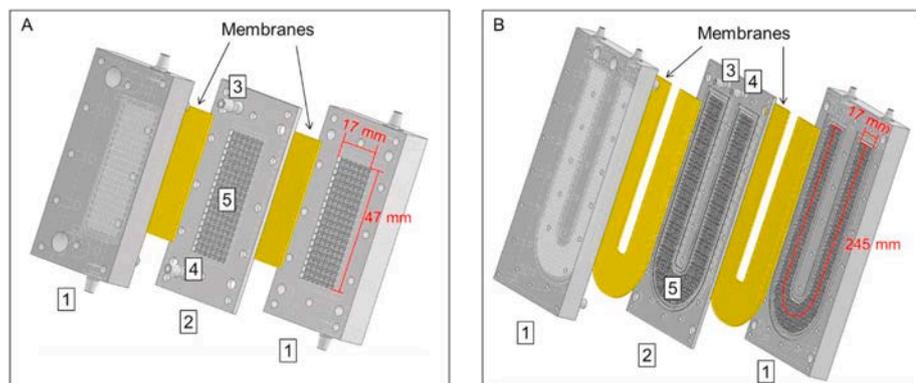
Fig. 1. Design of the 3D-printed membrane module for single pass UF/DF. (A) prototype module, (B) scaled-up module. 1: lateral parts for either diafiltration buffer or permeate solution; 2: middle part forming a flow pass for the feed, a membrane is placed between the middle part and the adjacent lateral part on both sides; 3: inlet of the feed flow; 4: outlet of the retentate flow; 5: hollow-carved grid structure to support the membranes. The width of the hollow-carved structure is the same in both modules (17 mm), while the length of the flow path in the scaled-up module is 5.2-fold larger than the one in the short prototype module.
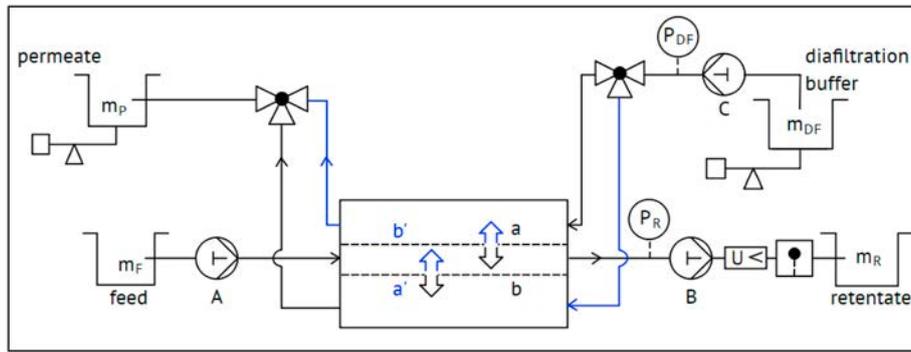
Fig. 2. Scheme of the experimental setup. The direction of the flows perfusing membrane a and b could be switched by means of the rotary valves of the FPLC system. The BSA and salt concentration in the retentate were monitored in real-time by UV and conductivity sensors, respectively.

FPLC system originally intended for the execution of salt gradients was used. The Akta software allows to precisely adjust the sum-flow of pump A and B and the ratio of how this sum-flow is distributed between the two pumps. If the ratio is selected as 1:1, saying the fraction of pump B is set to 50% of the sum-flow, the feed and retentate flows exactly match and the system is operated in pure diafiltration mode. Moreover, if the fraction of pump B is adjusted to less than 50% the system is able to

operate in a combined concentration/diafiltration mode. Exemplary concentration factors resulting from different settings of pump B are listed in the supplementary information (see SI Table S1). Besides the flows of the feed and retentate controlled by pumps A and B, the flow of the diafiltration buffer was controlled by the sample pump C of the Akta system. All flow rates were calibrated to the desired value before each experiment by collecting the corresponding effluent during a certain
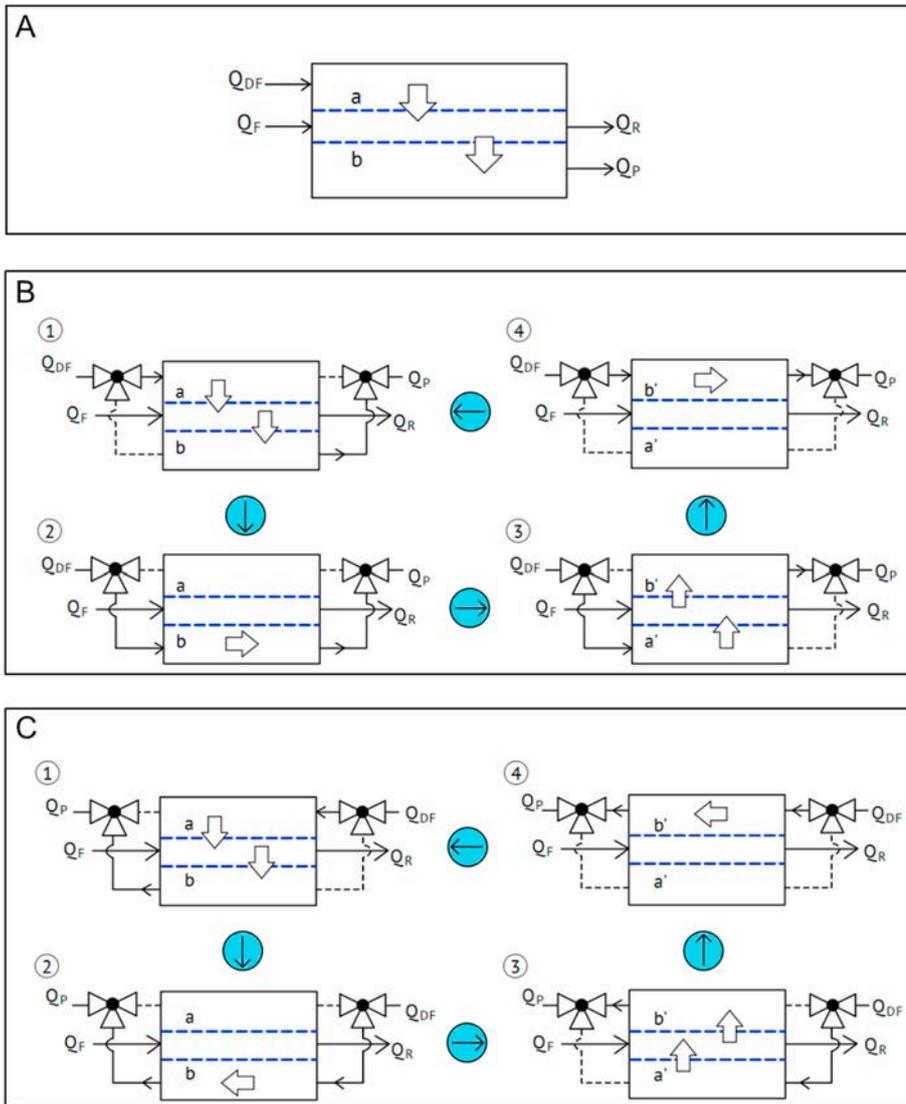
Fig. 3. Different continuous DF process modes controlled by switching the rotary valves. (A) Co-current diafiltration applying a unidirectional flow through membranes a and b, (B) Co-current diafiltration applying an alternating flow direction through membranes a and b, (C) Counter-current diafiltration applying an alternating flow direction through membranes a and b. The DF processes (B) and (C) can be executed with or without the flushing steps 2 and 4. The blue dashed lines indicate the membranes and the black dashed lines represent the flow paths which are blocked. (For interpretation of the references to colour in this figure legend, the reader is referred to the Web version of this article.)

3

period. BSA concentration was monitored at a wavelength of 280 nm, and diafiltration efficiency was calculated via the conductivity signal (see Fig. S1 in the supporting information). For the diafiltration process, fresh diafiltration buffer entered the middle part of the module at a constant flow rate and two rotary valves were applied to adjust the in- and outlet positions of the diafiltration buffer and the permeate at the lateral parts of the module. The pressures at the diafiltration inlet (P_{DF}) and the retentate outlet (P_R) as well as the weight of the diafiltration buffer and permeate reservoirs were monitored using the pressure sensors and scales of the Sartorius system. The developed process mode using an alternating permeate perfusion direction requires a repetitive switching of the valve positions and the flow rate of pump C. The corresponding process sequence was programmed using the software Unicorn 5.20 (GE Healthcare Bio-Sciences, Uppsala, Sweden).

2.4. Investigated diafiltration process modes

Different diafiltration studies were executed in order to explore the effect of varying stationary or alternating flow path onto the resulting diafiltration efficiency. First, the stationary two membranes unidirectional DF illustrated in Fig. 3A was tested. Through continuously pumping the exchange buffer perpendicular to the flow direction of the feed in the middle chamber, the limitations of this operation mode with unidirectional DF buffer flow were tested. In this mode, membrane a is constantly permeated with a fixed flow of fresh diafiltration buffer, while membrane b was constantly permeated by the solution flowing in the middle part, containing residues of the feed solution and fresh buffer.

Second, an alternating co-current diafiltration mode illustrated in Fig. 3B was investigated. This mode is characterized by a cyclic operation including the repeated use of four steps differing in the adjusted valve positions and resulting in different flow paths. In the first step the left rotary valve is adjusted to connect DF buffer to the inlet of the upper part of the module while the right valve blocks the outlet of this part. In consequence, the DF buffer is pumped from the upper to the middle part of the module. For plain diafiltration the feed and retentate flows are adjusted exactly at the same flow rate. Therefore, because of the conservation of mass, the permeation of the diafiltration buffer into the middle part enforces the same volume to permeate through membrane b. After a certain interval, the system switches to step 2 by changing the setting of the left valve defining the inlet position of the DF buffer. As a result, the flow path of the DF buffer is changed in a way that it simply flushes the lower part of the module in order to clean it from the permeate remaining after the end of step 1. In the third step, the setting of the right valve defining the position of the permeate outlet is changed in a way that it blocks the simple flushing of the lower part of the module and forces the DF buffer into the middle part crossing the first membrane (now named a' while being membrane b in step 1) and the permeate to cross the second membrane b'. By this the flow direction of the DF buffer is reversed sweeping away the concentration polarization layer formed by retained protein at membrane b (now a') surface during step 1. Finally, in step 4 the setting of the left valve is changed again, resulting in a flushing of the upper part of the module, having the same purpose than the flushing of the lower part during step 2. At the end of step 4, the cycle closes and by switching the setting of the right valve, the system enters a condition resembling the one of step 1. By switching the valves, the flow direction of the DF buffer is reversed again and the concentration polarization layer formed at the surface of membrane b' during step 3 is removed.

The third operation mode tested was an alternating counter-current diafiltration mode as illustrated in Fig. 3C. As can be seen, the four steps during a full process cycle of this mode resemble the ones of the cocurrent diafiltration mode with the difference that the flow direction of the DF buffer and permeate in the upper and lower part of the module is opposite to the flow direction of the retentate in the middle part. In this mode it was also tested if the flushing steps 2 and 4 can be skipped.

2.5. Analytical methods

For each diafiltration mode mentioned above, the sequential operating steps were executed repeatedly to approach a quasi-stationary state of the process. The achieved degree of buffer exchange is expressed as:

$$\text{Buffer exchange (\%)} \quad \left(1 \quad \frac{c_{Buffer,\,R}}{c_{Buffer,\,F}} \right) \cdot 100\% \tag{1}$$

where $c_{Buffer,R}$ and $c_{Buffer,F}$ are the concentrations of the initial buffer in the retentate and the feed (see Fig. S1). Two idealized physical models were used to predict the limits of buffer exchange. As shown in our previous work [20], the assumptions of ideal plug flow in all parts of the DF module and co-current flow direction result in an equation which is analogous to the well-known equation of constant volume diafiltration in a conventional TFF system [21], however, with the volumes of the initial feed and the used diafiltration buffer replaced by the respective volume flows:

$$c_{Buffer,R} \quad \left(c_{Buffer,F} \quad c_{Buffer,DF} \right) \cdot exp\left(\quad \frac{Q_{DF}}{Q_F} \right) + c_{Buffer,DF} \tag{2}$$

The second idealized model simply assumes complete mixing of the feed and the diafiltration buffer flows, as it is performed sequentially in the continuous diafiltration approach of Rucker-Pezzini et al. using several conventional SPTFF modules [6]. In this case the resulting concentration $c_{Buffer,\,R}$ is given by:

$$c_{Buffer,\,R} \quad \left(Q_F \cdot c_{Buffer,\,F} + Q_{DF} \cdot c_{Buffer,\,DF} \right) / (Q_F + Q_{DF}) \tag{3}$$

Besides, although the focus of our work was on continuous diafiltration, also the concentration factor (CF) of the used model protein BSA was defined using equation (4).

$$CF \quad \frac{c_{BSA,\,R}}{c_{BSA,\,F}} \tag{4}$$

where $c_{BSA,\,R}$ and $c_{BSA,\,F}$ is the concentration of BSA in the retentate and the feed, respectively. The main purpose of CF is to see the time course of BSA and the degree to which BSA is retained in the diafiltration module due to membrane fouling and/or concentration polarization.

3. Results and discussion

3.1. Co-current diafiltration with unidirectional permeate flow

The first test series was designed to verify the accuracy of the flow control of the developed system and to study the influence of the flow rate of the diafiltration buffer onto the degree of buffer exchange. In the experiments the small prototype module was used in co-current mode and unidirectional flow of the DF buffer and the permeate through the membranes. Both the feed and retentate flow rates were kept at $Q_F \quad Q_R$ 0.5 ml/min (56.4 L m^{-2} h^{-1}) over the course of the experiments, while increasing the diafiltration buffer flow rate Q_{DF} by 0.1 ml/min in every step from 0 to 0.5 ml/min. Standard deviations were analyzed by conducting every step in triplicates.

In the experiments the concentrations of BSA and buffer in the retentate, as well as the pressure in the middle part of the module were monitored during the continuous operation (see Fig. 4A–C). In addition, Fig. 4D shows the resulting buffer exchange and CF values for different flow rates of the diafiltration buffer Q_{DF}, and the theoretical values calculated using eq (1) and eq (4), respectively. The plot of the feed buffer content remaining in the retentate in dependence of the applied Q_{DF} shows the expected picture (Fig. 4A). If no diafiltration buffer is applied, the feed buffer concentration in the retentate shows a steep increase to the level of the buffer concentration in the inlet after a short delay determined by the residence time of the liquid in the middle part of the module. The steep increase also indicates that in this case the flow
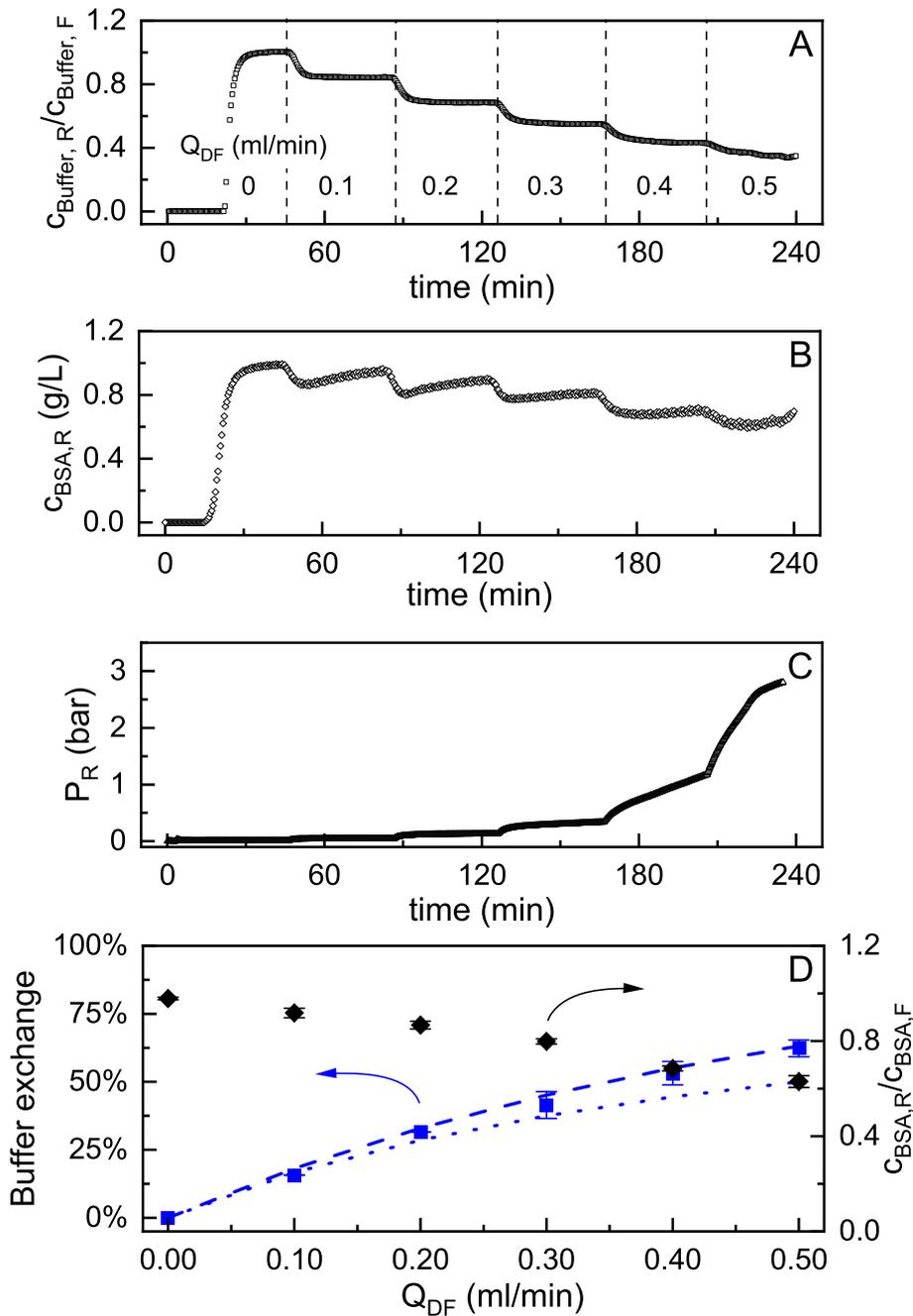
Fig. 4. Degree of buffer exchange of the co-current DF process with unidirectional flow through the membranes. In the course of the test series the flow rate of DF buffer was increased stepwise from 0 to 0.5 ml/min in steps of 0.1 ml/min, while the feed and retentate flow were kept constant at 0.5 ml/min. (A) Normalized concentration of the components of the original buffer remaining in the retentate, (B) Concentration of BSA in the retentate, (C) Pressure in the middle part of the membrane module, (D) Degree of buffer exchange and concentration factor of BSA plotted versus the flow rate Q_{DF}. The dashed lines represent the theoretical buffer exchange values corresponding to the idealized models of complete mixing (■ ■ ■ ■ ■) and plug-flow (▬ ▬ ▬), respectively.

profile in the middle part approximates an ideal plug flow. With increasing Q_{DF} the feed buffer concentration in the retentate starts to decline. By using accurate flow control of Q_F, Q_R, and Q_{DF} instead of the more common pressure control, the incompressibility of water enforces that the permeate flow through membrane b equals Q_{DF} in the case of the boundary condition $Q_F \quad Q_R$, which was applied in all experiments of Fig. 4. Together with the permeate flow a certain amount of the feed buffer is removed through membrane b resulting in the decreased level of this buffer in the retentate. However, Fig. 4B and C directly reveal the problems arising with the unidirectional flow through the membranes. During the initial period ($Q_{DF} \quad 0$) the BSA concentration in the retentate shows the expected steep increase. Because BSA is not able to penetrate the membranes and the ratio of $Q_R/Q_F \quad 1$ is not changed, in the ideal case, c_{BSA} would stay constant at this level throughout the complete experiment. That said, Fig. 4B shows that c_{BSA} deviates from this ideal behavior. After each increase of Q_{DF} the signal of c_{BSA} shows a

sharp dip followed by a slow return to the original level. Beyond Q_{DF} 0.2 mL/min the applied step duration is insufficient for the return, resulting in c_{BSA} in the retentate permanently staying below the feed level. In consequence BSA shows an ongoing accumulation within the module. This observation is consistent with the time course of P_R shown in Fig. 4C. During the initial steps ($Q_{DF} \quad 0$–0.3 ml/min) P_R stays at plateau levels below 0.3 bar, with the level of the plateau showing a small increase each time Q_{DF} is increased by 0.1 mL/min. The increase is caused by the simple fact, that after each step also the amount of permeate which has to penetrate membrane b is increased, requiring a larger transmembrane pressure (TMP). When Q_{DF} increased to 0.4 and 0.5 mL/min, the picture changes in a way, that within the monitored step duration no constant plateau of the pressure is reached, but the pressure displays a constant increase. This reveals that, besides the proportionally increased TMP required for higher Q_{DF}, an additional pressure drop results from the concentration polarization of BSA at the

surface of membrane b. Finally, the resulting buffer exchange is plotted in Fig. 4D and compared with the theoretical values calculated based on the plug flow as well as the complete mixing model (detailed values are shown in the SI part, Table S2). As can be seen, the experimental values lie between the two idealized models with a tendency to be closer to the plug flow results, something that can be expected to take into account the steep breakthrough observed in Fig. 4A. Nevertheless, the achieved buffer exchange of around 63% at Q_{DF}/Q_F 1 is too low to be of practical use. In order to achieve higher levels of buffer exchange, the flow of the diafiltration buffer must be increased further. Unfortunately, the attempt to follow this direction quickly leads to an inadmissible increase of the pressure within the middle part of the module.

3.2. Co-current diafiltration with alternating flow direction through the membrane

As described above, the use of a unidirectional permeate flow through membrane b of our module quickly resulted in a constantly rising pressure within the middle part of the module when the flow of the diafiltration buffer approached a ratio of Q_{DF}/Q_F around one. In order to avoid this problem, we introduced a single pass filtration with alternating flow direction of the diafiltration buffer. As in the case of the experiments described in section 3.1, the short prototype module was used and the flow rates of the feed Q_F and the retentate Q_R were adjusted at 0.5 ml/min (56.4 L m^{-2} h^{-1}) while the diafiltration buffer flow rate Q_{DF} was increased by 0.1 ml/min steps, starting at an initial value of 0.1 ml/min up to a maximum of 0.8 ml/min. Every parameter set was operated for 30 min, with a switching time of the alternating flow direction through the membrane of 10 min. After switching the inlet position of the diafiltration buffer, the remaining permeate was flushed with high flow rate of 10 ml/min for 10 s (for details see operation mode 'B' in Fig. 3, section 2.4). Since this operation mode resulted in a cyclic backflush of the accumulated concentration polarization layer of BSA, the signal detected by the UV sensor showed strong fluctuations. Hence, in order to get representative analytical results for each parameter set, the retentate was collected during the corresponding 30 min period and the average concentrations of BSA and feed buffer residues in the retentate were determined from this sample.

Fig. 5A shows the same trend of slowly decreasing residues of the feed buffer in the retentate with increasing Q_{DF}. However, the decrease does not show one clear step after increasing Q_{DF} by 0.1 ml/min, but a relatively smooth decrease superposed by a wiggle of the buffer concentration caused by the switching events of the alternating flow direction of the DF buffer. While this wiggle is relatively small in the case of the buffer concentration, it is much more pronounced for the BSA concentration in the retentate (Fig. 5B). Beyond a Q_{DF} of approx. 0.3 ml/min c_{BSA} in the retentate fluctuates between 0.6 and 1.3 g/L. Besides this short-term fluctuation, the average BSA concentration in the retentate is close to 1 g/L and therefore almost equal to the feed concentration. The minima of the concentration fluctuations show a slightly decreasing trend, which is likely caused by the fact that higher Q_{DF} result in a stronger concentration polarization during the 10 min intervals between the reversals of the DF buffer flow direction. Nevertheless, Fig. 5B is a first indication that the inherent backflushing caused by the cyclic reversal of the flow of the diafiltration buffer may result in the desired effect of limiting the accumulation of BSA within the filtration module. Looking at Fig. 5C it shows that also the pressure in the middle part of the module shows strong fluctuations in the case of higher Q_{DF}. Comparing the pressure peaks in Fig. 5C with the pressure plateaus in Fig. 4C one has to keep in mind that in Fig. 4 Q_{DF} increased stepwise to only 0.5 ml/min while in Fig. 5 the steps went up to a final diafiltration flow of 0.8 ml/min. Comparing the average pressure at Q_{DF} 0.5 ml/min in both experiments, the $\overline{P_R}$ values are 2.24 bar and 0.24 bar in the case of the unidirectional and the alternating flow direction of the diafiltration buffer. This shows that the alternating flow operation mode is

able to temporarily reduce the pressure build-up caused by the concentration polarization layer by sweeping this layer away. However, especially in the case of the highest Q_{DF} of 0.8 ml/min the reformation of the polarization layer at the opposite membrane after the switching event is quite fast, resulting in a pressure increase of more than 1.6 bar within a 10 min period. Finally, when looking at Fig. 5D, it must be concluded that the alternating DF flow operation mode did not result in an improved buffer exchange. Actually, in the case of the same Q_{DF} the buffer exchange of the alternating DF flow operation mode was even slightly less than the buffer exchange achieved with unidirectional DF flow mode (see SI Table S3). The explanation for this decrease is threefold. First, as can be expected, the alternating DF flow direction increases the mixing within the middle part of the module. Therefore, the buffer exchange moves closer to the lower boundary values given by the model assumption of complete mixing. Second, during the short flushing periods being part of the switching cycle, no diafiltration buffer enters the middle part of the module while the feed solution is continuously pumped into this region. And third, the flushing time of 10 s may not be long enough to remove all residues of the permeate. Therefore, in the initial phase after switching the flow direction the diafiltration buffer entering the middle part of the module may be contaminated by these residues. In conclusion, the results of Fig. 5 show that the alternating DF flow operation mode does not improve buffer exchange if the same parameters are applied as in the case of the unidirectional flow mode. However, the frequent reduction of the accumulated concentration polarization layer opens a wider window of possible operation parameters if the switching times are adjusted accordingly. In the next section, we discuss the results of different test series in which this parameter space was explored in order to find optimum operation conditions for the buffer exchange of our system.

3.3. Optimization of co-current diafiltration with alternating DF flow direction

The first parameter investigated was the flushing time applied for washing out the permeate residues from the lateral module part which serves for delivering the diafiltration buffer after the switching of the flow direction through the membranes. The investigated flushing times were 5, 10, 15 and 20 s while keeping the switching interval time at 10 min and the volume flows at Q_F Q_R Q_{DF} 0.5 ml/min (56.4 L m^{-2} h^{-1}). Each flushing parameter was investigated for 30 min, which means reversing the direction of DF flow for three times.

The experiments showed the highest buffer exchange of around 50% in the case of a flushing time of 15 s, and no significant difference of buffer exchange between 10, 15 and 20 s flushing time (see Table 2). When a flushing time of only 5 s was applied, the buffer exchange dropped significantly to 46%. Based on the hold-up volume of the section of the lateral module part which stays in contact to the membrane (1.25 ml) and the high flow rate during the flushing step (10 ml/min) the residence time of the liquid in this section can be approximated to 7.5 s. Therefore, a flushing time of 15 s corresponds to approx. two times the residence time and should guarantee an almost complete removal of permeate residues.

The next parameter investigated was the duration of the interval between the switching events of the DF flow direction. On the one hand, within long intervals the pressures in the module may approach a critical level. On the other hand, short intervals and frequent switching will increase the mixing in the module and the amount of DF buffer which is consumed for flushing. In order to investigate these relationships, we conducted two initial test series with increasing Q_{DF} (0.1 ml/min steps) applying switching intervals of 10 min and 5 min. Again Q_F and Q_R were kept constant at 0.5 ml/min. The respective Fig. S2 in the SI part shows that at low Q_{DF} the buffer exchange in the case of a switching interval of 5 min is slightly worse than the buffer exchange in the case of a switching interval of 10 min. This observation is within our expectation, because in the case of 5 min switching intervals the related detrimental
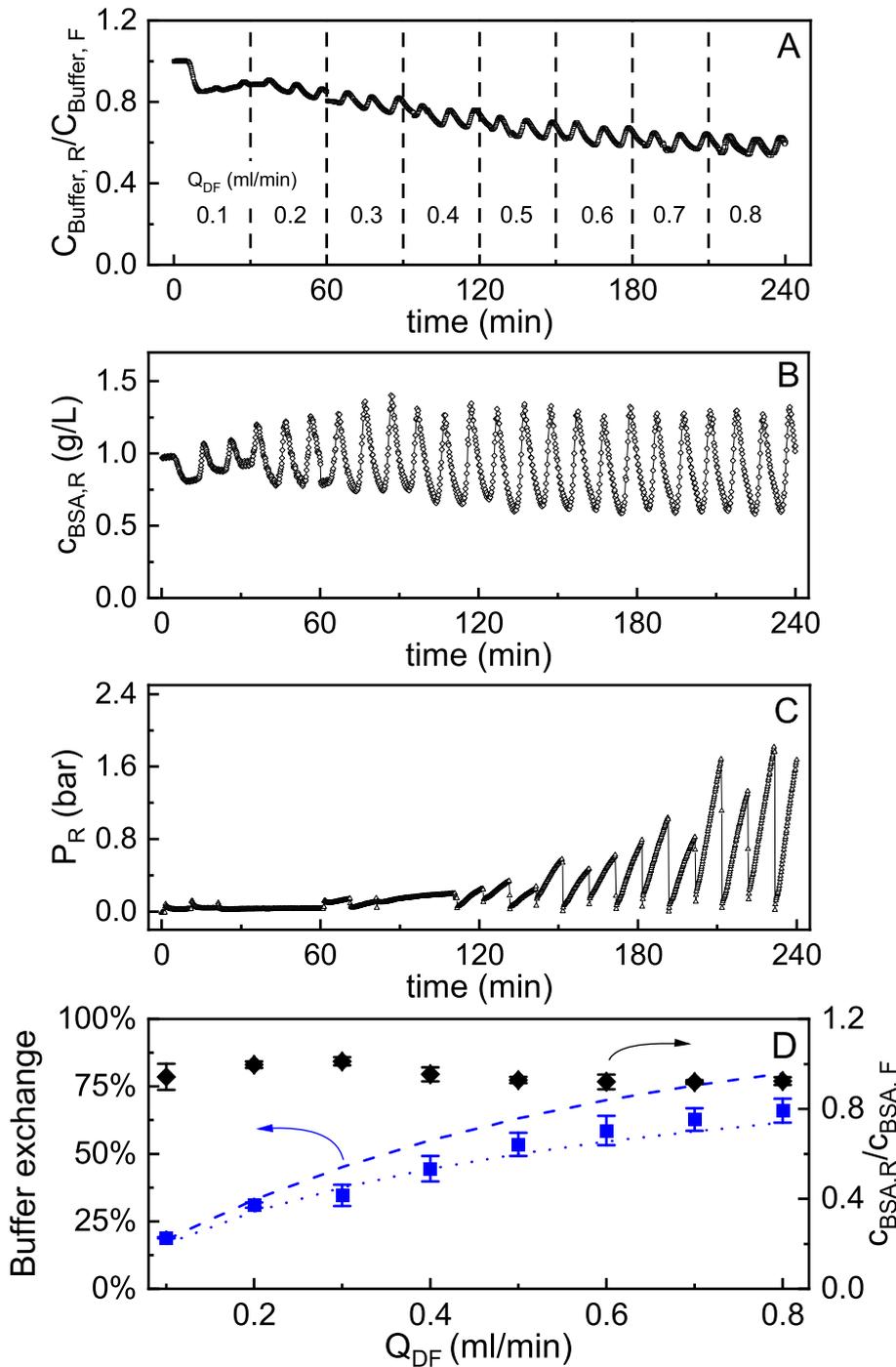
Fig. 5. Degree of buffer exchange of the co-current DF process with alternating flow direction through the membrane. In the course of the test series the flow rate of DF buffer was increased stepwise from 0.1 to 0.8 ml/min in steps of 0.1 ml/min, while the feed and retentate flow were kept constant at 0.5 ml/min. (A) Normalized concentration of the components of the original buffer remaining in the retentate, (B) Concentration of BSA in the retentate, (C) Pressure in the middle part of the membrane module, (D) Degree of buffer exchange and concentration factor of BSA plotted versus the flow rate of diafiltration buffer Q_{DF}. The dashed lines represent the theoretical buffer exchange values corresponding to the idealized models of complete mixing (■ ■ ■ ■ ■) and plug-flow (▬ ▬ ▬), respectively.

Table 2
Degree of buffer exchange as a function of flushing time.

Flushing time (s)	Buffer exchange	SD
5	45.8%	0.01
10	48.4%	0.03
15	48.8%	0.03
20	48.2%	0.004

effects, like mixing and short periods without diafiltration buffer entering the middle part of the module, occur more frequently. However, in the case of higher Q_{DF} values this trend seems to be reversed. A possible explanation for this effect is that in the case of higher Q_{DF} values

longer intervals between the flow reversals will lead to an enhanced concentration of BSA at the membrane surface. If BSA reaches very high concentrations it starts forming a gel like structure which hampers also the perfusion of hydrated ions and the sieving coefficient of the salt of the buffer drops below one, reducing the efficiency of buffer exchange.

Despite the small detrimental effect of short switching intervals, they offer the chance to increase Q_{DF} further. From our idealized plug flow model, it is known that a ratio of at least Q_{DF}/Q_F 7 is needed for a buffer exchange around 99.9%. Therefore, an experiment having a Q_{DF}/Q_F of 7.2 was conducted, in order to see how far the conditions of the co-current diafiltration with alternating DF flow can approach. Because the required Q_{DF} turned out to be too high in the case of Q_F 0.5 ml/min (56.4 L m^{-2} h^{-1}), we reduced the feed flow to 0.25 ml/min (28.2 L m^{-2}

h^{-1}) and adjusted Q$_{DF}$ at 1.8 ml/min. In addition, the switching interval was reduced to 3 min.

Fig. 6A shows the resulting time course of the buffer exchange for this experiment. Because of the reduced feed flow, the system requires a longer duration to approach quasi-stationary conditions, however, after 80 min a stable buffer exchange of around 92% could be achieved. This is the first time we succeeded to get a buffer exchange above 90% using the developed single pass filtration module. This enables potential applications having only moderate requests regarding the degree of diafiltration, such as reducing the salt content between two ion exchange chromatography steps. Besides the time course of the degree of buffer exchange, Fig. 6A also shows the pressures in the middle (P$_R$) and the lateral (P$_{DF}$) part of the module. Because of the short switching interval of 3 min, plotting the complete time course of the pressures results in a rather turbulent picture showing more than 70 narrow pressure peaks for P$_R$ and P$_{DF}$ (see Fig. S3 in the SI). Therefore, Fig. 6A only shows the average pressure values observed in each of the switching intervals. After an initial phase, the average pressure P$_R$ in the middle part approaches 2 bar with a very small incline during the duration of the experiment of 3.5 h. The pressure P$_{DF}$ in the lateral part of the module which is connected to the inlet of the diafiltration buffer is around 0.5 bar higher than P$_R$ and follows exactly the same trend. The consistency of the transmembrane pressure resulting from the difference between P$_{DF}$ and P$_R$ indicates, that the permeability of the membranes for pure diafiltration buffer stays constant and there is no permanent fouling of the membranes within the duration of the experiment.

3.4. Co-current diafiltration with alternating DF flow direction using a scaled-up module

While the increase of the Q$_{DF}$/Q$_F$ ratio to around 7 resulted in a clear improvement of buffer exchange, the value of 92% is still rather far from the theoretical optimum. Comparing our prototype module with other SPTFF modules, the very short flow path length of only 47 mm is an obvious difference hampering high buffer exchange. Therefore, the next stage in our stepwise optimization was the design of a scaled-up module having a flow path length of 245 mm. Using this new module, an experiment applying the same parameters (Q$_F$ ≈ Q$_R$ ≈ 0.25 ml/min; Q$_{DF}$ ≈ 1.8 ml/min) than the preceding one with the small module was conducted. In consequence, the feed flux per membrane area was reduced from 28.2 L/(m^2 h) to 5.05 L/(m^2 h), which is about 10 times less than conventional SPTFF systems used in multistep diafiltration. As can be seen in Fig. 6B, the buffer exchange in the scaled-up module increased to 95%, while using the same amount of diavolumes (7.2). More pronounced than this increase in buffer exchange is the strong drop in the maximum pressures achieved during the switching intervals, staying constant at P$_R$ ≈ 0.21 bar and P$_{DF}$ ≈ 0.35 bar throughout the experiment. Comparing these pressures with the ones appearing in the

small module, it can be seen that while the pressure difference between P$_{DF}$ and P$_R$ reduced only by approx. a factor of 3.6, the pressure in the middle part of the module (retentate chamber) dropped by almost a factor of 10. This shows, that besides the direct effect of the reduced specific flows, in the scaled-up module the pressure build-up in the middle part is also reduced due to a diminished concentration polarization. Again, detailed time courses of P$_{DF}$ and P$_R$ are displayed in the SI Fig. S3. It reveals, that in contrast of the time courses observed in the small module, the pressures in the scaled-up module reach a plateau after approx. 2 min and remain practically constant afterwards. Even when the diafiltration flux Q$_{DF}$ was further increased from 1.8 ml/min to 3.6 ml/min (14.4 DV), the pressure P$_{DF}$ in the module quickly reached a stable value of only about 1 bar. In case of this high diafiltration flux, the degree of buffer exchange reached up to 98.2% (see SI Fig. S4).

3.5. Counter-current diafiltration with alternating DF flow direction using a scaled-up module

For the unidirectional operation mode, as it is illustrated in Fig. 3A, the inlet position of the diafiltration buffer does not matter, because the complete upper lateral part of the module is filled with pure diafiltration buffer. However, in the case of the operation mode with alternating DF flow this situation changes. Now, after a switching event permeate residues are present in the lateral part which is entered by the diafiltration buffer, and the mutual alignment of the flow directions of Q$_F$ and Q$_{DF}$ makes a difference. From general engineering principles but also from the literature on single pass diafiltration [17,18] it is known that a counter-current design should have inherent advantages. Therefore, we explored the buffer exchange of our scaled-up module in case it is operated in counter-current mode with alternating DF flow direction, as it is explained in section 2.4 Fig. 3C. Three variants of counter-current DF were tested, differing in the application or the omission of the flushing step after switching the DF flow direction and the selected feed flow. The first two experiments were conducted under the same conditions: Q$_F$ ≈ Q$_R$ ≈ 0.25 ml/min, Q$_{DF}$ ≈ 3.6 ml/min at a switching interval of 3 min and a flushing flow rate of 26 ml/min for 15 s (if flushing was applied). For these operation conditions, the idealized models calculate theoretical buffer exchange of 93.5% and 100.0% in the case of complete mixing and plug-flow, respectively.

In the experiments applying counter-current mode with alternating DF flow direction the buffer exchange attained 99.7% with flushing steps applied (Fig. 7A). When compared with a corresponding experiment using exactly the same operation parameters but co-current flow (see SI Fig. S4) it shows that the performance of the counter-current mode is clearly better (99.7% compared to 98.2% buffer exchange). While the difference may not look very significant at first glance, one has to be aware, that this means that the retentate resulting from the co-current operation contained six times more (1.8%:0.3%) remaining
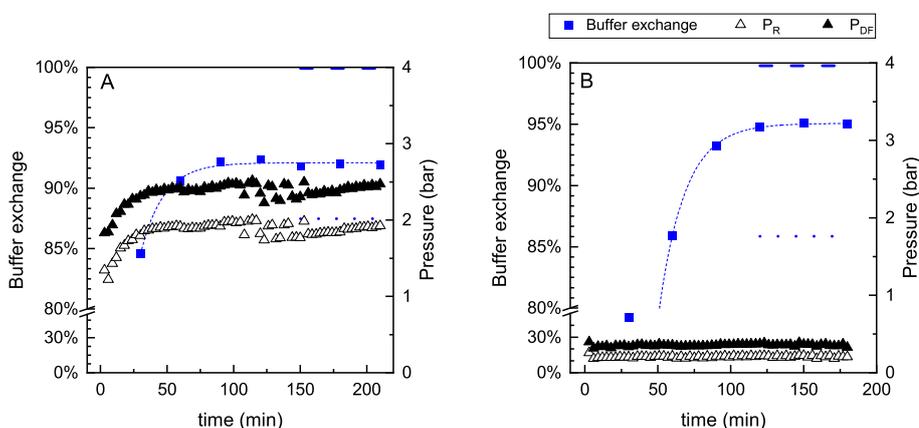
Fig. 6. Time course of the buffer exchange and the pressures in the middle (P$_R$) and the lateral (P$_{DF}$) part of the module for co-current diafiltration and alternating flow direction of the DF buffer through the membranes. The flushing time for the lateral part and the switching interval were 15 s and 3 min in both experiments. (A) small prototype module with a 5 cm flow path length, (B) scaled-up module with 25 cm flow path length. The dashed lines represent the theoretical buffer exchange value corresponding to the idealized models of complete mixing (■ ■ ■ ■ ■) and plug-flow (- - -), respectively.
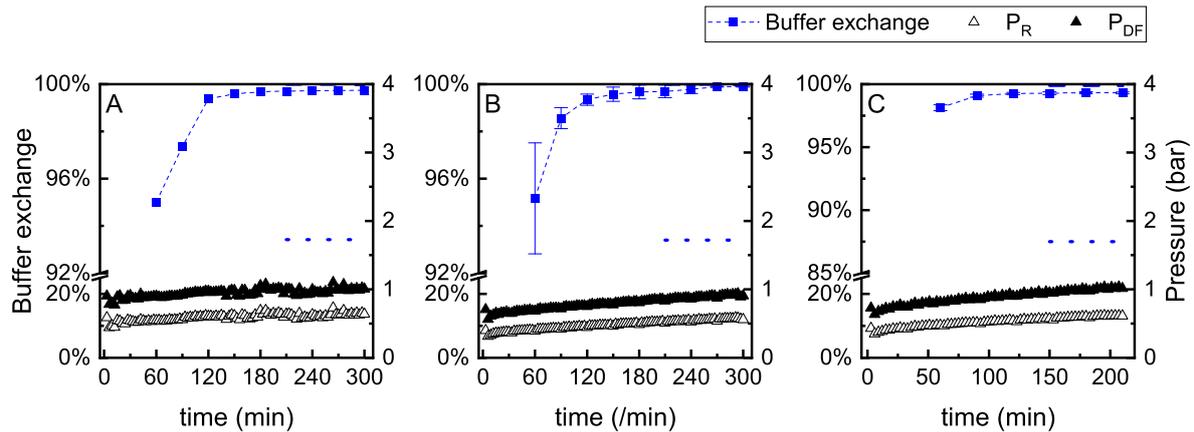
Fig. 7. Degree of buffer exchange and average pressures in the middle (P_R) and the lateral (P_{DF}) part of the module during the counter-current diafiltration with alternating flow direction of the DF buffer through the membranes. Q_{DF} = 3.6 ml/min, switching interval 3 min. (A) $Q_F = Q_R$ = 0.25 ml/min, with flushing steps applying 26 ml/min for 15 s, (B) $Q_F = Q_R$ = 0.25 ml/min, without flushing steps. (C) $Q_F = Q_R$ = 0.5 ml/min, without flushing steps.

'impurities' than the retentate resulting from the counter-current operation. When the intermittent flushing steps were omitted in the counter-current mode, the degree of buffer exchange even reached 99.9% (Fig. 7B). These results demonstrate the strong improvement that can be obtained if permeate residues in the lateral parts of the module are pumped towards the feed inlet because of the applied counter-current mode. Thus, if they penetrate back into the middle part after reversal of the DF flow direction, they dilute the high feed buffer concentration in the region of the feed inlet instead of contaminating the already desalted (diluted) solution close to the retentate outlet. The reason for the detrimental effect of the application of flushing steps is not fully understood yet. One possible explanation could be that the high volume flows occurring during the flushing result in an enhanced pressure gradient along the flow path in the respective lateral part of the module. In combination with the very low pressure in the middle part of the module during the flushing step[1] some unwanted circulating flows between the flushed lateral part and the middle part may occur, increasing axial dispersion and slightly reducing the buffer exchange. Another reason is that during the flushing step the actual diafiltration process in the middle part of the module comes to a temporary stop. Either way, the possibility to skip the flushing steps strongly simplifies the system control and saves the required volume of DF buffer. Taking the DF buffer used into account for flushing, the actual Q_{DF}/Q_F ratio of the experiment with flushing increases to 21.3, compared to 14.4 without flushing. Looking at the time course of the pressures, it shows that although the experiments ran for more than 5 h, the average value of P_{DF} and P_R showed only a slight increase and stayed below 1.1 bar in all cases. The maximum pressures occurring during the whole diafiltration process were less than 1.5 bar (see SI Fig. S5). Because the use of 14.4 diavolumes would result in a rather high buffer consumption in larger systems, we finally tested counter-current mode with alternating DF flow direction while switching back to the application of 7.2 diavolumes by doubling the feed flow. The resulting buffer exchange dropped slightly to 99.3% corresponding to a 140-fold removal of the impurities in the feed. If compared with the buffer exchange of a countercurrent staged diafiltration using several SPTFF units and the same amount of diavolumes (see Fig. 3 in Ref. [16]) it shows that our single 3D-printed membrane module achieves a buffer exchange being located between the ones of two- and three-stage SPTFF systems. It can be expected that after a further increase of the flow path length in our module, it will be able to challenge the buffer exchange of a three-stage SPTFF system in a

single device.

4. Conclusion and outlook

The experimental data presented in our study clearly show that the new design of a 3D-printed single pass filtration module housing two membranes is able to achieve diafiltration efficiencies up to 99.9% without the need of coupling several modules and/or intermediate dilution and mixing steps. For this achievement, the module design and its operation mode required a systematic stepwise optimization, leading to a system with 245 mm flow path length running in counter-current diafiltration mode with an alternating DF flow direction. Operating at 5–10 L/(m² h) the specific feed rate of our system is located between the corresponding values of commercial SPTFF systems [4] and the hollow fiber dialysis systems used by Yehl et al. [18]. Compared to our first paper, which reported the continuous diafiltration of BSA at feed concentrations of only 0.1 g/L, we increased the feed concentration tenfold in this work and preliminary experiments with higher concentrations indicate that the 3D-printed module also works fine at feed concentrations of 5 g/L. However, there is still another tenfold increase of the feed concentration needed in order to reach protein feed concentrations commonly applied during formulation. We expect that the module will be able to achieve high DF efficiencies also in this case, but it is likely that the specific feed rate has to be reduced to round 1–2 L/(m² h). Nevertheless, the productivity would stay in the range of around 25 g/(m² h), being in the same order of magnitude compared to the productivity reported by Yehl and Zydney (30 g/(m² h). Therefore, we think that our design might be suitable for cases in which small volumes must be diafiltrated and one wants to avoid the complexity of multi-stage SPTFF diafiltration, but also the large membrane area and hold-up volumes of the hollow-fiber system. The unconventional design of our system allows a cyclic reversal of the flow directions of DF buffer and permeate through the two membranes while continuously pumping the feed solution into the module. Thus, we can conduct an inherent back-flush in order to reduce the concentrated protein layer formed by concentration polarization at the membrane surface, during continuous operation. In future research we are going to test the limits of this approach regarding the admissible protein concentration in the feed, in order to demonstrate the suitability of the system at protein concentrations as they are encountered e.g. in the case of formulation steps during downstream processing.

CRediT author statement

Ruijie Tan: Conceptualization, Methodology, Visualization, Writing

---

[1] During the flushing $Q_F = Q_R$ still holds in the middle part and no permeate has to be pushed through the membrane. Therefore, P_R drops to practically zero.

References

[1] A.L. Zydney, Continuous downstream processing for high value biological products: a Review, Biotechnol. Bioeng. (2016), https://doi.org/10.1002/bit.25695.

[2] A. Jungbauer, Continuous downstream processing of biopharmaceuticals, Trends Biotechnol. 31 (2013) 479–492, https://doi.org/10.1016/j.tibtech.2013.05.011.

[3] A.L. Zydney, Perspectives on integrated continuous bioprocessing - opportunities and challenges, Curr. Opin. Chem. Eng. 10 (2015) 8–13, https://doi.org/10.1016/j.coche.2015.07.005.

[4] J. Dizon-Maspat, J. Bourret, A. D'Agostini, F. Li, Single pass tangential flow filtration to debottleneck downstream processing for therapeutic antibody production, Biotechnol. Bioeng. 109 (2012) 962–970, https://doi.org/10.1002/bit.24377.

[5] N.A. Bleckwenn, H. Golding, W.E. Bentley, J. Shiloach, Production of recombinant proteins by vaccinia virus in a microcarrier based mammalian cell perfusion bioreactor, Biotechnol. Bioeng. 90 (2005) 663–674, https://doi.org/10.1002/bit.20423.

[6] J. Rucker-Pezzini, L. Arnold, K. Hill-Byrne, T. Sharp, M. Avazhanskiy, C. Forespring, Single pass diafiltration integrated into a fully continuous mAb purification process, Biotechnol. Bioeng. 115 (2018) 1949–1957, https://doi.org/10.1002/bit.26708.

[7] A. Vancleef, S. Seurs, J. Jordens, T. Van Gerven, L.C.J. Thomassen, L. Braeken, Reducing the induction time using ultrasound and high-shear mixing in a continuous crystallization process, Crystals 8 (2018), https://doi.org/10.3390/cryst8080326.

[8] S. Xu, J. Gavin, R. Jiang, H. Chen, Bioreactor productivity and media cost comparison for different intensified cell culture processes, Biotechnol. Prog. 33 (2017) 867–878, https://doi.org/10.1002/btpr.2415.

[9] A. Arunkumar, N. Singh, M. Peck, M.C. Borys, Z.J. Li, Investigation of single-pass tangential flow filtration (SPTFF) as an inline concentration step for cell culture harvest, J. Membr. Sci. 524 (2017) 20–32, https://doi.org/10.1016/j.memsci.2016.11.007.

[10] C. Casey, T. Gallos, Y. Alekseev, E. Ayturk, S. Pearl, Protein concentration with single-pass tangential flow filtration (SPTFF), J. Membr. Sci. 384 (2011) 82–88, https://doi.org/10.1016/j.memsci.2011.09.004.

[11] D. Barba, F. Beolchini, D. Cifoni, F. Veglió, Whey protein concentrate production in a pilot scale two-stage diafiltration process, Separ. Sci. Technol. 36 (2001) 587–603, https://doi.org/10.1081/SS-100102948.

[12] J.C. Martínez-Alvarado, B. Torrestiana-Sánchez, M.G. Aguilar-Uscanga, Isolation of steviol glycosides by a two-step membrane process operating under sustainable flux, Food Bioprod. Process. 101 (2017) 223–230, https://doi.org/10.1016/j.fbp.2016.11.013.

[13] A. Simon, L. Vandanjon, G. Levesque, P. Bourseau, Concentration and desalination of fish gelatin by ultrafiltration and continuous diafiltration processes, Desalination 144 (2002) 313–318, https://doi.org/10.1016/S0011-9164(02)00333-8.

[14] F. Lipnizki, J. Boelsmand, R.F. Madsen, Concepts of industrial-scale diafiltration systems, Desalination 144 (2002) 179–184, https://doi.org/10.1016/S0011-9164(02)00309-0.

[15] J.C. Te Lin, A.G. Livingston, Nanofiltration membrane cascade for continuous solvent exchange, Chem. Eng. Sci. 62 (2007) 2728–2736, https://doi.org/10.1016/j.ces.2006.08.004.

[16] A.M.K. Nambiar, Y. Li, A.L. Zydney, Countercurrent staged diafiltration for formulation of high value proteins, Biotechnol. Bioeng. 115 (2018) 139–144, https://doi.org/10.1002/bit.26441.

[17] M.G. Jabra, C.J. Yehl, A.L. Zydney, Multistage continuous countercurrent diafiltration for formulation of monoclonal antibodies, Biotechnol. Prog. 35 (2019) 6–11, https://doi.org/10.1002/btpr.2810.

[18] C.J. Yehl, M.G. Jabra, A.L. Zydney, Hollow fiber countercurrent dialysis for continuous buffer exchange of high-value biotherapeutics, Biotechnol. Prog. 35 (2019) 1–5, https://doi.org/10.1002/btpr.2763.

[19] C.J. Yehl, A.L. Zydney, Single-use, single-pass tangential flow filtration using low-cost hollow fiber modules, J. Membr. Sci. 595 (2020) 117517, https://doi.org/10.1016/j.memsci.2019.117517.

[20] R. Tan, M. Franzreb, Continuous ultrafiltration/diafiltration using a 3D-printed two membrane single pass module, Biotechnol. Bioeng. (2019), https://doi.org/10.1002/bit.27233.

[21] H. Lutz, Ultrafiltration for bioprocessing. https://doi.org/10.1016/B978-1-907568-46-6.00002-1, 2015, 244.